DESIGN ORIENTED METHODS FOR ASSESSMENT OF ACCIDENTAL EXPLOSION EFFECTS

Jørgen Amdahl

Department of Marine Technology, Norwegian University of Science and Technology

ABSTRACT

The accuracy of single degree of freedom analysis of the response to accidental explosions is investigated. Maximum displacements for beams and stiffened plates predicted with simplified methods are checked by comparison with results of nonlinear finite element analyses using beam and shell modeling. The simplified methods are adopted by the NORSOK Standard N-004 for design against accidental explosions, and the effect of some recent improvements of the formulations are checked. The ductility limit given in NORSOK is verified, by comparing strains that can be derived from the criterion with strains from finite element shell analysis

INTRODUCTION

Adequate design against accidental explosions is essential in the offshore industry as well as in many other industries and sectors. The design is traditionally based upon simplified methods. Notably, the so-called Biggs' method [1] has become very popular. Biggs' approach is based upon a single degree of freedom (SDOF) idealisation of the fairly complicated non-linear response to an explosion. This facilitates fairly simple estimates to be made of the maximum displacement of a structural component.

Today, the development of computers and algorithms has made possible advanced analysis with the nonlinear finite element method (NLFEM) of structural members and subsystems. This eliminates most of the simplifying assumptions that has to be made in the Biggs'- or other methods. However, it is generally not a trivial task to perform nonlinear analysis, e.g. the modelling, and execution of the analysis is often demanding with respect to both man-hours and skills.

The simplified methods warrant therefore, still their existence; notably for screening of the severity of the explosion scenarios, reserving NLFEM for the critical cases. Every designer working with NLFEM should have knowledge of the method, allowing him/her to check the validity of the NLFEM results. Consequently, design requirements based on simplified methods remain in many design codes, e.g. both the Interim Guidance Notes (IGN) [2] and the NORSOK Standard N-004 [3] for steel offshore structures exposed to accidental actions.

The purpose of the present work is to check the accuracy of SDOF methods, notably the approach adopted in NORSOK. A revision of this code is underway, and the effect of the modifications proposed is particularly studied. It should also be mentioned that Det Norske Veritas is in the process of developing a Recommended Practice (RP) for design against accidental actions [4]. This RP will be based upon the revised NORSOK N-

004, but will also include a section of design philosophy as well as some very recent achievements. In recognition that it is often challenging to use the proposed method for designers who are not very familiar with the subject, the RP will contain several worked-out examples on the use of the methods to realistic problems in the Commentary sections.

SDOF SYSTEM ANALOGY

Biggs assumed that the structure under action of the dynamic pressure pulse - ultimately attains a deformed configuration comparable to the static deformation pattern. Using the static deformation pattern as displacement shape function, the dynamic equations of equilibrium can be transformed to an equivalent single degree of freedom system, expressed as:

$$\left(k_{lm,u}M_u + k_{lm,c}M_c\right)\ddot{y} + K(y)\,y = F(t) \qquad \textbf{(1)}$$

where $k_{lm,u}$ and $k_{lm,c}$ are the load-mass transformation factor for uniform mass, and concentrated mass, $k_{m,u}$ and $k_{m,c}$ are the corresponding mass transformation factors for uniform mass and concentrated mass, k_ℓ is the load transformation factor. M_u and M_c are the total uniform mass and concentrated mass, F is the total load and K is the characteristic stiffness.

For a *linear system*, the load mass factor and the characteristic stiffness are constant $K = K_1$. For a *non-linear system*, the load-mass factor and the characteristic stiffness depend on the response (deformations). The resistance is often modelled as bi-linear. The response can then be expressed in terms of: K_1- characteristic stiffness in the initial, linear resistance domain, Y_{el}- displacement at the end of the linear resistance domain and T - eigenperiod in the initial, linear resistance domain

For a given explosion load history the maximum displacement, y_{max}, is found by analytical or numerical integration of equation (1). For standard load histories and standard resistance curves maximum displacements are presented in design charts for various ratios of the limit resistance, R_{el} (corresponding to the formation of a plastic mechanism) and the maximum explosion pressure, F_{max}. When the duration of the pressure pulse relative to the eigenperiod in the initial, linear resistance range is known, the maximum displacement, y_{max}, normalised against y_{el} for a given R_{el}/F_{max} is determined from the diagram as illustrated Figure 1 for a triangular pressure pulse.

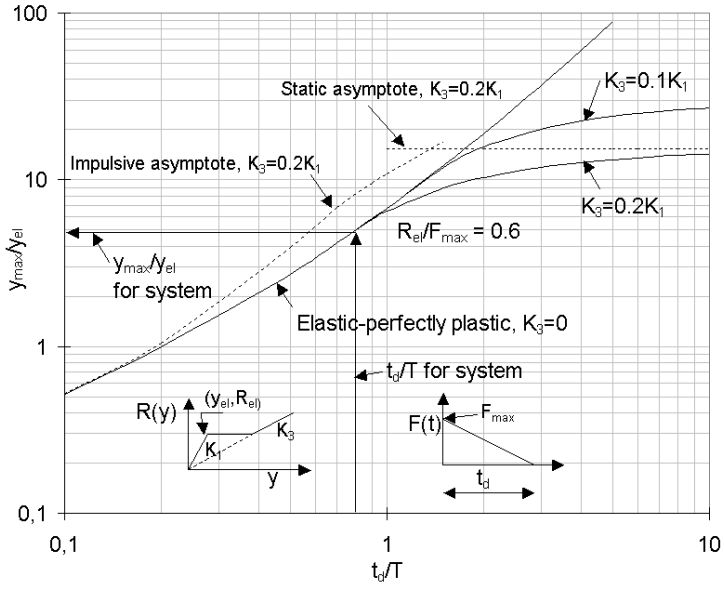

Figure 1 Response chart for an SDOF system with bi-linear and tri-linear resistance function

An extension to the Biggs' method introduced in NORSOK in the sense that response charts for systems with resistance functions exhibiting strength increase in the large displacement range are provided. This strength increase could be due to membrane action, strain hardening etc., or a combination of these effects. The

strength increase is idealised as a third deformation phase with constant stiffness K_3 as illustrated in Figure 1. It is observed that the maximum displacement for such systems ($K_3 > 0$) will be bounded, by contrast to systems with a purely bi-linear resistance.

The Biggs' method considers members that deform by bending, only. For members with small length to height ratio, shear deformation may become important, notably for members that can be considered as clamped at the boundaries (e.g. stiffeners subjected to uniform pressure over several frame spacings). In the forthcoming revision of NORSOK a modification of the resistance function in the linear region and the associated eigenperiod due to shear deformations is proposed.

BEAM ANALYSIS - SDOF MODEL VS. NLFEM

I-profile beams

The shear effect model outlined above is verified against NLFEM analyses with the space-frame program USFOS [5] for beams with different I-cross-sections. The cross-sectional dimensions of the beam, which is 3 m long, are shown in Figure 2a. For simplicity only the height of the profile is changed, keeping the other dimensions constant. The yield stress of the material is f_y = 300 MPa.

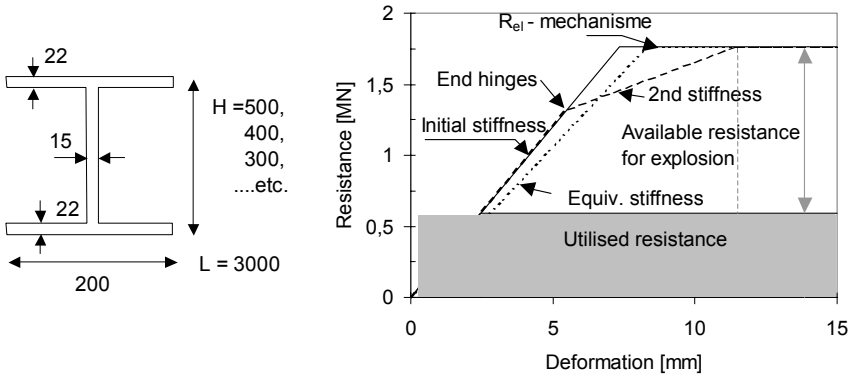

(a) (b)

Figure 2 a) I-profile dimensions b) Resistance function for the example beam with two masses.

In order to check the accuracy of the proposed formulations results from SDOF analyses are compared with simulations using the nonlinear finite element program USFOS. The beam concept in the program contains nonlinear geometry effect, and nonlinear plasticity is modeled with plastic hinges. In order to avoid obscuring the effect of shear flexibility, any effect of shear on the plastic bending moment is not taken into account. The ends of the beam are clamped, but free to move inwards, so no membrane action is generated. The resistance function is therefore considered to be bi-linear. Strictly, a tri-linear resistance function should be used, because plastic hinges are created at the ends of the beam prior to the mid hinge, whereby the stiffness in the last phase up to R_{el} is greatly reduced. Instead, the stiffness expression used, except for a few cases, is the so-called equivalent stiffness that preserves the "true" energy dissipation in the resistance up to R_{el}. These principles are illustrated Figure 2b. The explosion load is assumed to be uniformly distributed. The pressure pulse is triangular with duration 13.8 msecs and equal rise – and decay time. The maximum pressure is varied.

The results of the study are summarized in TABLE 1. The maximum deformations obtained with the SDOF model and NLFEM are presented as ductility ratios, scaled against the limit of the elastic range, y_{el}. y_{el} depends on whether it is calculated form pure bending considerations or whether the effect of shear deformations is included.

It appears that the ductility ratios predicted depend significantly on whether shear is included or not, notably for small L/H ratios. When L/H = 6, the ductility predicted from pure bending is in the order of twice as large as that predicted when shear is included. It is observed, however, that the ductility ratios obtained with the SDOF model and the NLFEM is not very different (regardless of whether shear is included or not), except for ductility ratios close to 1. This means that the maximum deformation (in absolute terms) is predicted

fairly well using a bending model. This is somewhat surprising, and leads to the conclusion that the results are relatively insensitive to the stiffness used in the elastic range, so long there is a correct correspondence between the elastic stiffness and the eigenperiod, and the ductility ratio $\mu >> 1$. It is fair to say, though, that the shear model performs slightly better as far as maximum deformation is concerned. The most important effect is, however, that the model predicts the elastic stiffness, the elastic limit (y_{el}) and hence the ductility ratio, significantly better than the bending model. This is confirmed by the NLFEM analyses.

TABLE 1

DUCTILITY RATIOS FOR BEAM SUBJECTED TO EXPLOSION LOAD

L/H		15			10				7.5				6			
F_{max} [MN]		1.77	1.98	2.52	2.94	3.36	3.96	4.68	2.94	4.11	4.92	5.52	2.94	5.52	5.88	7.62
R_{el} [MN]		1.41			2.34				3.42				4.62			
R_{el}/F_{max}		0.80	0.70	0.55	0.80	0.70	0.59	0.50	1.17	0.83	0.70	0.62	1.57	0.84	0.79	0.60
w_{max}[mm]		41	71	174	33	68	147	274	6.2	31	76	134	3.9	31	46	169
Bending	t_d/T	2.3			3.5				4.6				5.6			
	μ_{1DOF}	3.2	8.2	22.4	4.8	11.8	27.1	61.1	0.9	3.7	19.6	39.7	0.7	5.2	9.5	66.0
	μ_{1DOF} *	3.7			4.3				0.7	4.5			5.3			
	μ_{NLFEM}	5.2	9.1	22.2	6.4	13.3	28.7	53.3	1.6	7.9	19.6	34.7	1.3	10.0	14.8	54.2
B&Shear	t_d/T	2.0			2.7				3.3				3.7			
	μ_{1DOF}	2.6	7.7	18.5	2.7	7.1	19.7	42.3	1.0	3.4	10.2	19.2	0.7	3.8	6.2	29.5
	μ_{1DOF} *	2.8			2.9				0.8	3.1			3.5			
	μ_{NLFEM}	3.9	6.8	16.8	4.1	8.6	18.6	34.5	0.9	4.4	10.9	19.4	0.6	4.8	7.2	26.3

* Ductility calculated with bi-linear stiffness in elastic region

For both models the use of an equivalent stiffness yields a maximum deformation that deviate significantly from the NLFEM results for small ductility ratios ($\mu < 5$), although the model that includes shear is better. Some results with the SDOF model are therefore also presented using the correct stiffness prior to and after formation of end hinges. The accuracy is then greatly improved. This implies that it could be worthwhile to perform accurate numerical simulations rather than using design charts for subjected to uniformly distributed explosion loads and small permissible ductility ratios.

Beam with two concentrated masses

The beam studied is the I-profile with web height equal to 0.3 m. The beam is clamped, but free to move axially. It is assumed that two concentrated masses, $3 \cdot 10^4$ kg each, representing say mounted equipment, are positioned at L/3 from the ends. This yields a utilisation of 0.33 with respect to the limit resistance, R_{el}. The limit resistance corresponds to formation of a complete plastic mechanism, which occurs at a displacement y_{el} = 11.5 mm; virtually identical for the NLFEM analysis and the SDOF model with the shear effect included. The eigenperiod of the beam is 89.3 msecs using SDOF modelling, compared to 93.2 msecs from NLFEM.

Assume that the beam is subjected a total explosion load of 3.25MN with a duration of 50 msecs and equal rise and decay time. The explosion load is first assumed distributed as two concentrated loads at the location of the concentrated masses (L/3 lengths). The maximum deformation according to NLFEM simulations is 48.1 mm.

In the SDOF analysis, the available resistance, R_{el}, has to be reduced by 1/3 due to the static utilisation caused by the gravity forces from the two masses, refer Figure 2b. This yields an effective $R_{el}/F_{max} = 0.36$. Using the equivalent stiffness for bending and shear for two concentrated loads, the SDOF model predicts 43.4 mm maximum deformation. This is not bad considering that the effective stiffness in the linear phase should be smaller than the one used, because of the static utilisation.

If the resistance in the linear range is modelled bi-linearly prior to and after formation of end hinges as indicated in Figure 2b, there is obtained 46.5 mm maximum deformation.

In the above analysis the explosion pressure is lumped as two concentrated loads at L/3 from the ends. In many cases the pressure is transmitted to the beam from stiffeners such that modelling it as a uniformly distributed load is often more appropriate. With a uniform load distribution it is found that the same amount of deformation (48.1 mm) is obtained with a maximum total load of 4.58 MN. Hence, the beam has a significantly larger capacity than that predicted by the concentrated load model (3.25 MN). A major reason for the discrepancy is that the load factor for the concentrated load is 0.8 versus 0.53 if the load is uniformly distributed.

Assume that an average load factor could be calculated according to the relative contribution from the two concentrated loads (static = 0.59 MN) and the distributed load (4.58 MN). This gives a load factor of 0.56. Hence, the total load from the lumped model (3.25 MN) should be multiplied by 0.8/0.56 = 1.43, giving 4.64 MN. This result is quite close to the NLFEM value.

ANALYSIS OF PLATE-STIFFENER

The next problem to be studied is the accuracy of SDOF and beam modeling of stiffened plating. The results from non-linear analysis based on a shell finite element representation are assumed to give the most correct answer. The shell element used is the one developed by Haugen and Skallerud [6]. The plate is assumed to be 1.8 m long and 0.6 m wide, with an aspect ratio of three. The stiffener is a T-profile and the dimensions are varied as indicated in Figure 3. The length of the stiffener is 3.0 m. The stiffener is assumed welded to transverse girders, such that the profile shape is preserved at the ends. This is modeled with high stiffness beam elements at the ends of the shell model.

It is assumed that the ends are clamped against rotation and either fixed or free axially. Symmetry conditions are imposed on the long edges of the plates. In addition, the edges are assumed to be constrained, i.e. the edges remain straight, but are free to move in. This is ensured by introducing springs with large in-plane shear stiffness on the long edges. The shell finite element model I shown in Figure 3. A single analysis is also performed with the refined mesh that is indicated.

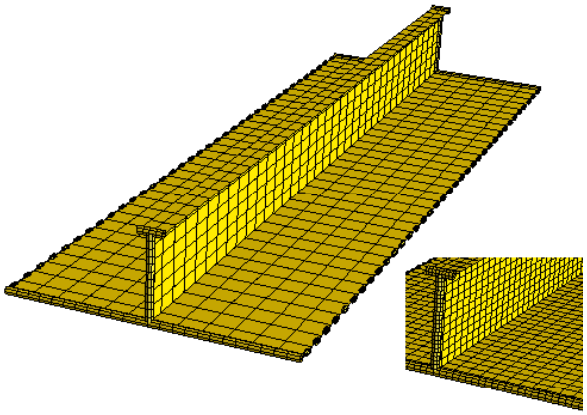

	Case 1	Case 2	Case 3
Web height	0.180	0.180	0.120
Web thickness	0.012	0.008	0.006
Top flange width	0.050	0.050	0.050
Top flange thickness	0.012	0.012	0.010
Plate flange width	0.600	0.600	0.600
Plate flange thickness	0.012	0.008	0.006

Figure 3 Shell element model of plate-stiffener - stiffener dimensions

The static resistance for the three cases is plotted in Figure 4a-c, which shows the resistance scale factor versus lateral displacement. (A scale factor of 1.0 corresponds to a uniform pressure of 1.06 MPa). For the shell model plots are provided for both the stiffener at mid-span as well as for the plate midway between stiffeners at midspan. It is observed that the plate deforms significantly relative to the stiffener initially, but as the stiffener collapses, the relative deformation decreases. The resistance predicted by the beam model is somewhat softer than resistance of the shell model using the stiffener displacement, but the agreement is generally quite good. The resistance curves that can be derived from NORSOK (§A.6.9.2) underestimate clearly the onset of membrane stiffening when the ends are fixed axially. This model is based upon a three-hinge mechanism approach, which does not describe accurately the displacement field for uniformly distributed loads. Fortunately, the use of such resistance functions is conservative.

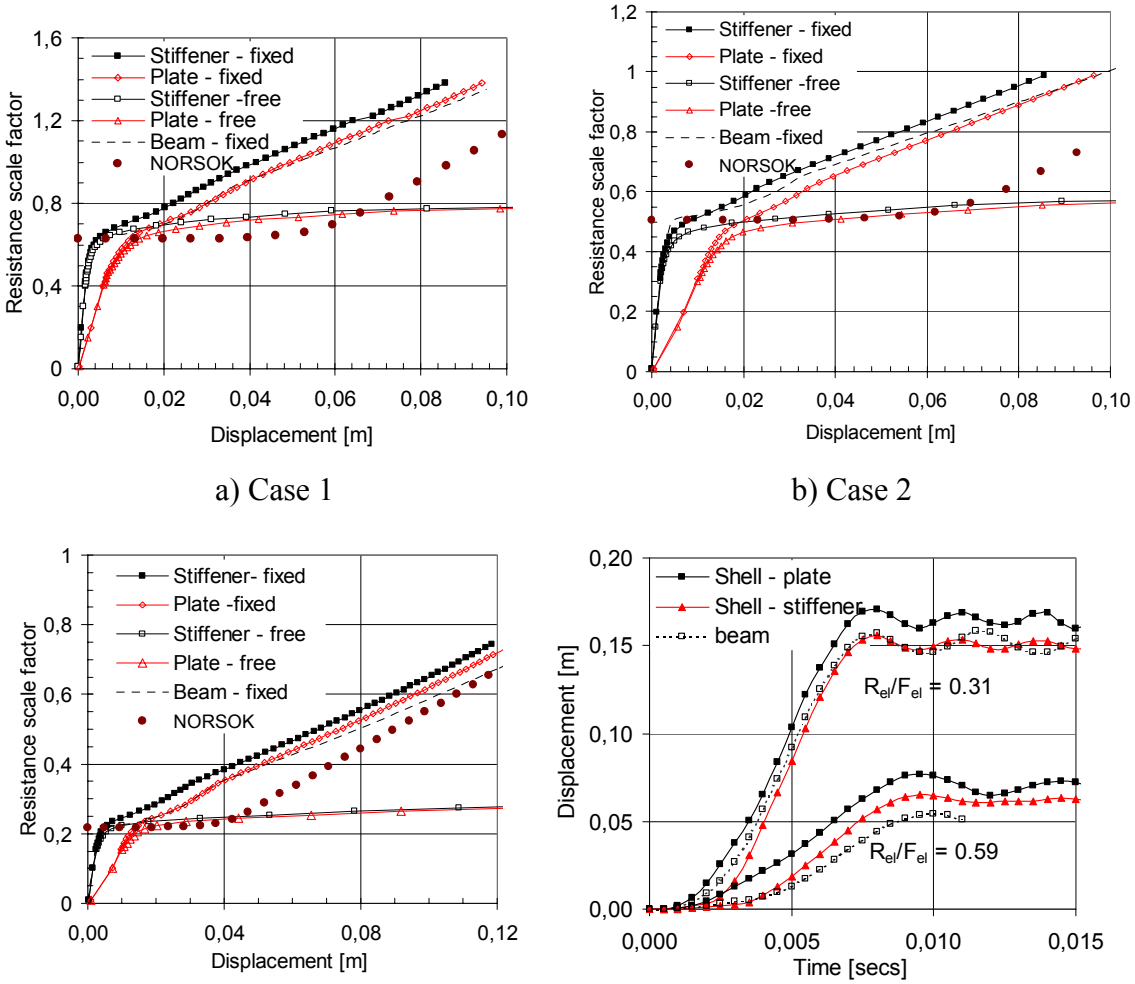

Figure 4 Static resistances for Cases 1 - 3 and examples of dynamic response for Case 2**.**

TABLE 2

MAXIMUM DISPLACEMENT FROM NLFEM SIMULATIONS AND SDOF MODEL

	Duration 8.3 msec			Duration 15 msec		
	Case 1	Case2	Case 3	Case 1	Case2	Case 3
Max.load factor F_{max}	1.5	1.5	0.5	1.0	0.8	0.5
Resistance R_{el}	0.63	0.47	0.22	0.63	0.47	0.22
R_{el}/F_{max}	0.42	0.31	0.44	0.63	0.59	0.44
t_d/T	2.34	2.47	1.79	4.2	4.5	3.22
Shell	85 mm	156 mm	64 mm	48 mm	65 mm	89 mm
Beam	92 mm	157 mm	64 mm	50 mm	55 mm	102 mm
1DOF	92 mm	185 mm	58 mm	43 mm	63 mm	71 mm

Dynamic analyses are carried out for stiffener/plate axially fixed and subjected to explosion pulses with duration 8.3 msecs and 15 msecs. The pressure pulse is triangular, and the rise time is 30% of pulse duration. The maximum load factor is varied as shown in TABLE 2. The temporal variation of the mid-span displacement for the Case 2 simulations is shown in Figure 4d. For this case the displacements obtained with the beam model and the shell model are in excellent agreement for the large response, but differ by ~15% for the small response.

TABLE 2 shows that the beam model is capable of predicting the maximum displacement with satisfactory accuracy for the other cases as well.

Finally, the predictive capability of the SDOF model is investigated by numerical integration of the differential equation. In this study the resistance functions for the plate-stiffeners are based upon a bi-linear representation of the static resistance functions simulated with the shell finite element model as shown in Figure 3. The eigenperiods are estimated using beam relationships. From TABLE 2 it is observed that the maximum displacements are similar to those simulated with NLFEM. This confirms that the SDOF model performs satisfactory provided that the resistance function is representative for the real response. Obviously, because the resistance functions given for stiffened plates in NORSOK underestimate the static resistance (refer Figure 4a-c), the response to explosion loads will be overestimated if the NORSOK resistances are used.

DUCTILITY LIMIT

A very important issue in conjunction with designing against explosions is the level of deformation that can be assumed prior to disintegration of the member. Various ductility limits are specified in codes. In particular, NORSOK offers a ductility limit (§A.3.10.4) that is intended for application on resistance curves derived from NLFEM or simple plastic methods based on the plastic hinge concept.

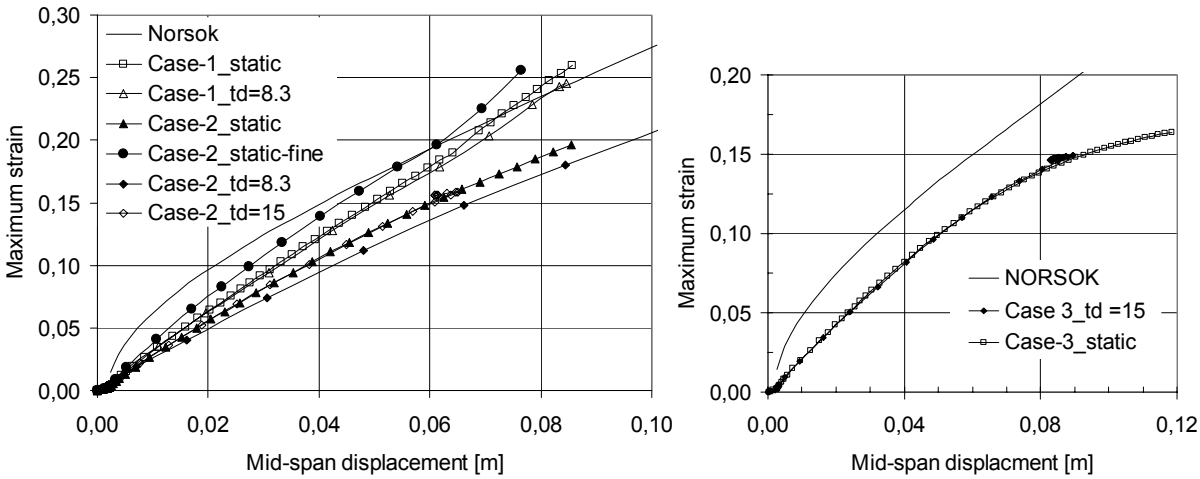

Figure 5 Maximum strain versus mid-span displacement for plate-stiffener

Figure 5 shows the relationships between maximum strain (≡ critical strain for rupture) and mid-span displacement (denoted NORSOK), which can be derived from the NORSOK criterion, for three cases of plate-stiffener. For Case 1 and Case 2 plate-stiffener the criterion is virtually equal. The strains predicted in the NLFEM simulations are plotted in the same diagrams. It is observed that the strains from the static shell analyses agree quite well with those obtained in the dynamic analyses, although a small dynamic dependence is evident for Case 2. A single analysis is performed with the refined mesh for Case 2. While the resistance curves show very little sensitivity to the mesh fineness considered, it appears that the fine mesh yields a noticeable increase in the predicted strain. Figure 5 shows that NORSOK ductility relationship performs quite well. Except for the fine mesh at large deformation, the strain that is derived from the criterion is conservative compared to those of the NLFEM simulations, notably for intermediate levels of strain. It should be noticed that elastic displacements are not included in the NORSOK criterion. It is not unreasonable to add the elastic displacement to the value given by the criterion, if the resistance curve includes elastic displacements.

It is a difficult to say what mesh fineness that should be the required. The NORSOK code acknowledges at least the sensitivity of the strain predictions to mesh fineness and specifies that the critical *average membrane* strain for a shell element in NLFEM shell analysis of axially loaded plate material, in lieu of more accurate considerations, should be taken as

$$\varepsilon_{max} = 0.02 + \frac{0.65}{\ell/t} \qquad \ell/t \geq 5 \tag{2}$$

where ℓ is the length of element shorter side and t is thickness of plate. In the present case is $\ell/t < 5$ for both meshes, so the same ductility limit will apply.

CONCLUSIONS

Comparisons with the results of NLFEM beam analyses have shown that SDOF METHODS can provide very satisfactory estimates of the response to accidental explosions, provided that the governing physical effects are represented in the resistance functions. As concerns prediction of the *maximum absolute deformation*, correct modelling of the stiffness in the linear elastic range is not so important, provided that the ductility ratio μ is large and the calculated eigenperiod corresponds to the stiffness assumed. However, the calculated ductility ratios may be false and criteria for permissible ductility ratios should be used with care.

For short, clamped members shear deformation has a pronounced effect on both the initial stiffness and eigenperiod. Very satisfactory prediction of the maximum deformation is obtained with SDOF models including the shear effect. This constitutes therefore an improved basis for ductility considerations.

It is shown that beam modelling of a plate-stiffener performs quite well when compared with results of NLFEM shell analysis. The static resistance of the beam is very similar to the one obtained for the shell, while the simple methods underestimates the resistance. If the static resistance from NLFEM analysis is used as input, the SDOF method works very well.

The resistance the plate-stiffeners studied seem to be invariant with respect to the size of the element mesh actually used. However, for a given case, the strain is clearly mesh size dependent. The NLFEM strains are compared with the strain level that can be derived from the ductility criterion given in NORSOK. It seems that the NORSOK criterion constitutes a reasonable "upper bound" for a plate-stiffener.

REFERENCES

1. Biggs, J. M (1964) *Introduction to Structural Dynamics*, McGraw Hill, New York

2. Interim Guidance Notes for the design and Protection of Topsides structures against Explosion and Fire, SCI-P-122, The Steel Construction Institute, 1991.

3. NORSOK Standard N-004 (1998) Design of Steel Structures Appendix A - Design against Accidental Actions, Norwegian Technology Standard Institution, Oslo

4. Recommended Practice No. DNV-RP-C204 Design against Accidental Loads, Draft 2002 (In progress), Det Norske Veritas, Høvik.

5. Eberg E., Hellan Ø. and Amdahl, J. (1993). Nonlinear Reassessment of Jacket Structures under Extreme Storm Cyclic Loading- Part III: Development of Structural Models for Cyclic Response, 12th Int. Conf. Offshore mechanics and arctic Eng. , OMAE '93, Glasgow

6. Skallerud, B. and Haugen, B. (1999). Collapse of Thin Shell Structures – Stress Resultants Plasticity Modelling within a Co-Rotated ANDES Finite Element Formulation, Int. J. Numerical Methods Engng., vol 36, pp 1961 – 1986.